



# Determination of 16 polycyclic aromatic hydrocarbons in seawater using molecularly imprinted solid-phase extraction coupled with gas chromatography-mass spectrometry

Xingliang Song<sup>a,b,1</sup>, Jinhua Li<sup>b,1</sup>, Shoufang Xu<sup>b,d</sup>, Rongjian Ying<sup>a</sup>, Jiping Ma<sup>c</sup>, Chunyang Liao<sup>b</sup>, Dongyan Liu<sup>b</sup>, Junbao Yu<sup>b</sup>, Lingxin Chen<sup>b,\*</sup>

<sup>a</sup> School of Chemistry & Chemical Engineering, Linyi University, Linyi 276005, China

<sup>b</sup> Key Laboratory of Coastal Zone Environmental Processes, Yantai Institute of Coastal Zone Research, Chinese Academy of Sciences, Chunhui Road 17, Laishan District, Yantai 264003, China

<sup>c</sup> Key Laboratory of Environmental Engineering of Shandong Province, Institute of Environment & Municipal Engineering, Qingdao Technological University, Qingdao 266033, China

<sup>d</sup> Graduate University of Chinese Academy of Sciences, Beijing 100049, China

## ARTICLE INFO

### Article history:

Received 8 April 2012

Accepted 30 April 2012

Available online 21 May 2012

### Keywords:

Polycyclic aromatic hydrocarbons

Molecularly imprinted polymers

Solid-phase extraction

Seawater samples

Sol-gel process

Gas chromatography-mass spectrometry

## ABSTRACT

A method of solid-phase extraction (SPE) using molecularly imprinted polymers (MIPs) as adsorbent coupled with gas chromatography-mass spectrometry (GC-MS) was developed for the determination of 16 types of polycyclic aromatic hydrocarbons (PAHs) in seawater samples. The MIPs were prepared through non-covalent polymerization by using the 16 PAHs mixture as a template based on sol-gel surface imprinting. Compared with the non-imprinted polymers (NIPs), the MIPs exhibited excellent affinity towards 16 PAHs with binding capacity of 111.0–195.0  $\mu\text{g g}^{-1}$ , and imprinting factor of 1.50–3.12. The significant binding specificity towards PAHs even in the presence of environmental parameters such as dissolved organic matter and various metal ions, suggested that this new imprinting material was capable of removing 93.2% PAHs in natural seawater. High sensitivity was attained, with the low limits of detection for 16 PAHs in natural seawater ranging from 5.2–12.6  $\text{ng L}^{-1}$ . The application of MIPs with high affinity and excellent stereo-selectivity toward PAHs in SPE might offer a more attractive alternative to conventional sorbents for extraction and abatement of PAH-contaminated seawater.

© 2012 Elsevier B.V. All rights reserved.

## 1. Introduction

Polycyclic aromatic hydrocarbons (PAHs), among the group of persistent organic pollutants (POPs), have received great concerns in recent years because of their high lipophilicity, carcinogenicity and ubiquitousness in the environment [1–5]. The prolonged accumulation of PAHs has posed severe threats to the environment and human health. So, identification and measurement of PAHs has become a topical task. Generally, gas chromatography-mass spectrometry (GC-MS) is the most frequently used analytical technique for PAHs [4–6]. However, because of the complexity of matrix and low content of PAHs, high efficiency clean-up and enrichment procedures are required prior to analysis [6–8]. Various pretreatment processes for the extraction and concentration of PAHs from water samples have been increasingly developed, such as liquid-phase

microextraction (LPME) [9], solid-phase extraction (SPE) [10,11], stirring bar sorptive extraction (SBSE) [12], and solid-phase microextraction (SPME) [13]. SPE, due to its advantages [10,14], has been widely employed for concentration of PAHs in water samples [10,11,15,16]. Meanwhile, it is well known that low selectivity and low adsorption capacity are existing main problems associated with traditional sorbents of SPE. A new type of high efficiency sorbent, molecularly imprinted polymers (MIPs), owing to high sample load capacity, high selectivity, high mechanical and thermal stability, low cost and easy preparation, have been increasingly used (e.g. SPE sorbent) for preconcentration and high efficient separation of various trace analytes in diverse matrices [17–21], based on their unique imprinting and recognition properties.

On the other hand, it is well known that PAHs are a class of highly lipophilic compounds without any pronounced functional groups in their molecules, and the non-covalent interactions like hydrogen bond, dipolar and/or ionic interactions between PAHs and functional monomer cannot be formed. So, it seems most difficult to imprint PAHs since the only available interactions in the imprinting and recognition process are the hydrophobic

\* Corresponding author. Tel./fax: +86 535 2109130.

E-mail address: lxchen@yic.ac.cn (L. Chen).

<sup>1</sup> Equally contributed to this work.

interaction, steric cavity, and  $\pi$ - $\pi$  interaction, which are one or two orders of magnitude weaker than the electrostatic forces [22]. To the best of our knowledge, only several publications have reported PAHs determination based on MIPs by using PAHs as template/analyte. For instances, Benzo[a]pyrene (BaP) was used as a template molecule to synthesize six kinds of MIPs using different functional monomers and cross-linkers for enrichment and separation of BaP from water and coffee samples [23], as well as, pyrene was used as a template molecule to prepare MIPs with molecular recognition properties towards many PAHs [24]. The double molecular imprinting for measurements of PAHs in water was performed with quartz crystal microbalance [25]. Besides, the double template imprinting was employed for dispersive solid-phase microextraction and attained satisfactory cleanup and enrichment efficiency for three PAHs in seawater [26]. The multi-molecular imprinting technique was proposed that the MIP-particles were prepared by using six PAHs mix as a template, and successfully applied for selective adsorption of PAHs [27,28]. Furthermore, the MIPs-SPE with five-PAH mix as template was employed, and thereby highly sensitive determination of PAHs in ambient air dust was attained by GC-MS [29]. However, most of the fabrication processes used above in molecularly imprinting is still complex, removing the template is difficult, and the kinetics of the sorption/desorption process is often unfavorable [18,30,31].

To solve these problems, surface imprinting [30,31] has been used herein, and an ultrathin polymer coating on a solid support substrate through the surface imprinting approach can conduce to easy removal of template as well as improved mass transfer of PAHs. A multi-molecular imprinting approach for PAHs was demonstrated, based on a surface imprinting sol-gel process. The MIPs sorbents were synthesized in acetonitrile by using 16 PAHs mix standards as a template, phenyltrimethoxysilane as the functional monomer, and tetraethoxysilane as the cross-linker. Numerous binding cavities were produced in the polymer matrix because of the advantages of PAHs with condensed benzene rings and non-reactivity between PAHs molecules. Binding selectivity and matrix effects of the MIPs were investigated in detail. The molecularly imprinted SPE (MISPE) was successfully applied to enrich 16 PAHs from spiked samples such like artificial and natural seawater.

## 2. Experimental

### 2.1. Materials and instrumentation

Sixteen standard PAHs, i.e., naphthalene (Nap), acenaphthylene (Acy), acenaphthene (Ace), fluorene (Fl), phenanthrene (Phe), anthracene (Ant), fluoranthene (Flu), pyrene (Py), benz[a]anthracene (BaA), chrysene (Chr), benzo(b)fluoranthene (BbF), benzo[k]fluoranthene (BkF), benzo[a]pyrene (BaP), indeno[1,2,3-cd]pyrene (IPy), dibenz[a,h]anthracene (DahA) and benzo[ghi]perylene (BghiP), nominated as priority pollutants by United States Environmental Protection Agency (EPA), dissolved in methylene dichloride, were purchased from Supelco (Bellefonte, PA, USA), individual at 2000 mg L<sup>-1</sup>. The related information such as structures and physicochemical properties of the 16 PAHs can be found in our previous work [9]. Stock solutions at the concentration of 10 mg L<sup>-1</sup> were prepared in acetonitrile, and working solutions were prepared daily by appropriate dilution of the stock solutions with seawater before use. Silica gel (400–600 mesh, Qingdao Ocean Chemical Co., Qingdao, China) was used as the carrier of MIPs. Phenyltrimethoxysilane (PTMS) and tetraethoxysilane (TEOS), obtained from Tianjin Chemical reagent Co. Ltd (Tianjin, China), were used as functional monomer and cross-

linker, respectively. Acetonitrile (HPLC grade, Tianjin Chemical, Tianjin, China) was used as solvent, and acetic acid (analytical grade, Ji'nan Chemical, Ji'nan, China) was used as polymerization initiator. Acetone (analytical grade, Laiyang Xinglin Chemical Co., Ltd, Laiyang, China), methanol (HPLC grade, Ji'nan Friend Chemical Co., Ltd, Ji'nan, China) and dichloromethane (DCM) were used for elution of the template. Other affiliated chemicals and materials were all obtained from Sinopharm Chemical Reagent Co. Ltd. (Shanghai, China) and local suppliers (Linyi, China). All other solvents and reagents were of analytical grade and used without further purification. Doubly deionized water (DDW) obtained by a Milli-Q Ultrapure water system (Shanghai Yarong Instrument Co., Ltd, Shanghai, China) was used throughout the experiments.

GC/MS QP 2010 coupled with a split/splitless injector system and a quadrupole mass spectrometer (Shimadzu, Japan) was used for separation and determination of PAHs. High-speed Centrifuge (G16-WS, Hunan Xiangyi Laboratory Instrument Development Co., Ltd, China) was employed for centrifugation. Super Digital Display Thermostatic Bath (SYC-15, Nanjing, China) was used for heating. Vacuum Drying Chamber (DZF-6051, Nanjing, China) was used for drying of MIPs. Solid Phase Extraction Vacuum Manifolds (Mate-24, Shanghai Quandao Technical Company, Shanghai, China) was employed for SPE process. Digital Full-Temperature Oscillator (HZQ-2, Jiangsu Jintan Medical Instrument Factory, China) was used for oscillation.

### 2.2. Preparation of molecularly imprinted sol-gel adsorbent

The procedure for activating the silica gel (400–600 mesh) was referred to that reported in reference [32] with necessary modification. The MIPs sorbent was synthesized in a 250 mL glass vessel using 25 mL acetonitrile as a solvent. 500 mg mL<sup>-1</sup> 16 standard PAHs solution (1 mL) and 5.0 mL PTMS were dissolved in acetonitrile, then the mixture was incubated for 30 min at 5 °C in a water bath. Into the activated silica gel (1.0 g), TEOS (4 mL) and acetic acid (2.00 mL) were added and stirred for another 20 min. The acetic acid was used as a polymerization initiator (2.0 mL), while PTMS was used as a functional monomer, TEOS as a cross-linking agent and the 16 standard PAHs as template molecules. The mixture was incubated while stirring at 400 rpm for 24 h at 60 °C in a water bath. The resulting particles were collected on a glass filter, washed extensively with 50 mL of methanol overnight continuously, washed with 15 mL of methanol for 1 h, and dried at 100 °C for 12 h. Cleaned beads were extracted by DCM in a Soxhlet extractor, and this procedure was repeated until the template molecules could not be detected in the washed solvent by GC-MS. The corresponding non-imprinted polymers (NIPs) were prepared in parallel in the absence of template and treated in the same manner.

### 2.3. Characterization of the polymers

The prepared polymers were characterized by scanning electron microscopy (SEM), nitrogen adsorption experiments and Brunauer-Emmett-Teller (BET) analysis, Fourier transform infrared spectroscopy (FT-IR) and gas chromatography-mass spectrometry (GC-MS).

SEM images were recorded using a scanning electron microscope (SEM, Hitachi S-4800, operating at an accelerating voltage of 5 kV and a magnification 200000 ×). All samples were sputter-coated with gold before SEM analysis.

Nitrogen adsorption-desorption results were recorded using AUTOSORB 1 (Quantachrome Instruments, Germany). The BET method was used to determine the specific surface area, performing for N<sub>2</sub> relative vapor pressure of 0.05–0.3 at 77 K. The samples

were degassed in a vacuum at 300 °C prior to adsorption measurements.

FT-IR spectroscopic measurements were performed on model Avatar 370 FT-IR Spectrometer (Thermo Nicolet Corporation, USA) with KBr pellet method. The wave numbers of FT-IR measurement range were controlled from 500 to 4000  $\text{cm}^{-1}$ , and collected at one data point per 2  $\text{cm}^{-1}$  with sample scanning for 32 times.

GC–MS conditions employed for PAHs separation and determination were as follows: a quadrupole mass spectrometer was operated in the electron ionization mode at 70 eV and mass spectra were acquired with a selected ion monitoring (SIM) mode. Separation was carried out on a Rtx-5MS capillary column (30 m  $\times$  0.25 mm) with a 0.25  $\mu\text{m}$  stationary film thickness, 95% methyl-5% phenyl copolymer column (Shimadzu, Tokyo, Japan). The oven temperature was programmed as follows: initial 70 °C (held for 2 min), increased to 90 °C (held for 4 min), afterwards increased to 290 °C at a rate of 10 °C  $\text{min}^{-1}$ , and eventually held for 20 min. The total time for one GC run was 44 min. The injector temperature was set at 250 °C, and the injection was performed in a splitless mode for 1 min. Helium (purity 99.999%) was employed as carrier gas at a flow rate of 1.0  $\text{mL min}^{-1}$ .

#### 2.4. Adsorption capacity of the polymers

To evaluate the adsorption capacity of the obtained polymers, a dynamic adsorption test and a static adsorption test for PAHs were carried out in the artificial seawater and natural seawater samples, respectively. By monitoring the temporal amount of PAHs in the solutions, the procedures of the dynamic adsorption test were performed as follows: 50 mg of MIPs were dissolved in 10 mL of seawater spiked with 2  $\mu\text{g L}^{-1}$  individual PAH standards, and then the mixture was continuously oscillated in a thermostatically controlled water bath at room temperature for 1–24 h; the polymers were removed centrifugally, and then the 5 mL of supernatant was extracted by using dispersive liquid-liquid microextraction (DLLME) procedure [9,33,34] into a 10 mL glass-centrifuge tube; and then the analytes were located in the bottom of the tube, 1  $\mu\text{L}$  of which was sampled for GC–MS analysis. For each adsorbent, these experiments were repeated at least triplicates.

Meanwhile, the static adsorption test was carried out by allowing a weighted amount of MIPs to reach the equilibrium (the adsorption equilibrium would be obtained within 20 h) with PAHs standard solution of known concentration from 1.0 to 10.0  $\mu\text{g L}^{-1}$ . The same procedure was used to test the adsorption amounts of NIPs.

Equilibrium amounts of PAHs bound to the MIPs ( $B$ ) were calculated by the following equation:

$$B = \frac{(F_0 - F_t)V}{W}$$

where,  $F_0$  and  $F_t$  are the concentrations ( $\mu\text{g L}^{-1}$ ) of PAHs measured at initial and after interval time for equilibrium, respectively;  $V$  and  $W$  are the volumes of the PAHs solution and the weight of the dried polymers used for the binding experiments, respectively.

#### 2.5. Molecularly imprinted solid-phase extraction (MISPE) procedure

The polymers of 0.15 g were packed into an empty SPE cartridge of 3.0 mL (purchased from Agilent Technologies, USA) between two PTFE frits with 10  $\mu\text{m}$  in porosity size. Prior to loading the sample, the cartridge was washed with a mixture of DCM/acetic acid (9:1, v/v) until PAHs could not be detected by GC–MS in the filtrate, and then 5 mL artificial seawater was used for

activation. A 30.0 mL seawater solution spiked with a known concentration of PAHs was percolated through the MIPs or NIPs cartridge. The cartridge was washed with 2.0 mL methanol/ $\text{H}_2\text{O}$  (1:9, v/v). Then the analytes were eluted from the cartridge by using 2.0 mL of DCM/acetic acid (9:1, v/v) for five times. This fraction was then collected and concentrated up to 0.5 mL under an ice-water bath in nitrogen stream. One microliter (1  $\mu\text{L}$ ) samples were analyzed by GC–MS to quantify the recovered PAHs.

### 3. Results and discussion

#### 3.1. Preparation and characterization of MIPs for PAHs

Non-covalent molecular imprinting method was adopted to prepare MIPs for PAHs. Theoretically, the imprinting effect of MIPs towards its template mainly depends on the interaction between the template and the functional monomer. PAHs are poly-electronegative molecules with condensed benzene rings, and have no distinct functional groups. So, PTMS as functional monomer was employed for the imprinting and recognition process, possibly owing to the hydrophobic interaction and  $\pi$ - $\pi$  interaction. The weakly polar acetonitrile was chosen as porogen because strongly polar solvents could counteract the formation of affinity bonds for templates, and acetic acid was chosen as the activator during the synthesis of molecularly imprinted sol-gel [35]. Thus, the imprinting process of PAHs regularly encoded the PAH shape of -SiO-SiO-SiO- conjoined to a functional phenyl group, and the specific cavity was formed after the imprinted molecule was eluted.

Fig. 1 shows the FT-IR spectra of activated silica gel (curve a), non-imprinted silica gel (curve b) and imprinted silica gel (curve c). As seen in Fig. 1a, the strong peaks at 469, 800 and 1102  $\text{cm}^{-1}$  can be attributed to the stretching vibration of Si-O-Si, indicating the formation of silica gel; the broad peaks at 3439 and 1637  $\text{cm}^{-1}$  might represent the stretching vibration of the

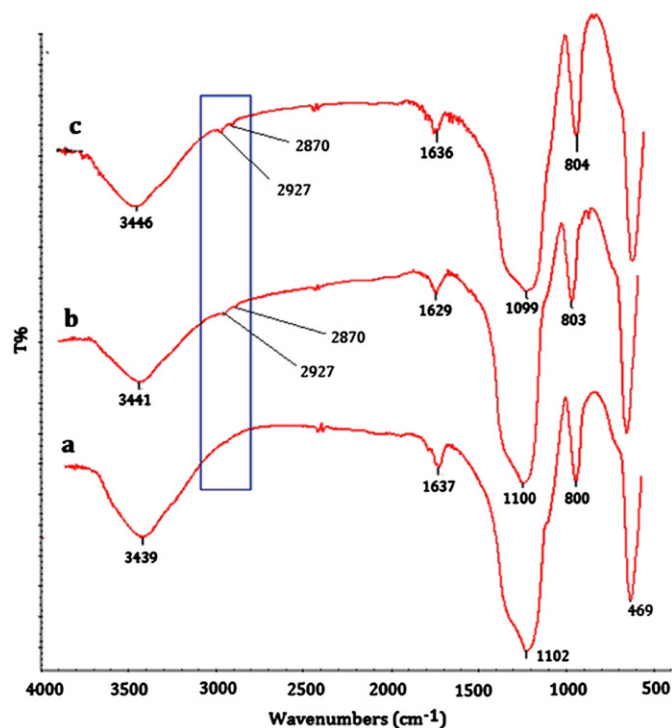


Fig. 1. SEM images of (a) activated silica gel, (b) non-imprinted silica gel and (c) imprinted silica gel.



associating hydroxyl and the bending vibration of hydroxyl of the silica gel, respectively [36]. As illustrated in Fig. 1b and c, the peaks at 2927 and 2870  $\text{cm}^{-1}$  can be assigned to the stretching vibration of C–H of methyl; the weak absorbance peak nearby 1636  $\text{cm}^{-1}$  showed the appearance of skeleton vibration absorption of benzene-ring from the non-imprinted and imprinted silica gel. These observations suggested that PTMS was successfully grafted to the surface of silica gel and the thinner silica films were fabricated in MIPs and NIPs, respectively, according to the weak signals judgment. Additionally, the hydroxyl bending vibration peaks near 3446  $\text{cm}^{-1}$  (Fig. 1c) in MIPs showed obvious blue shift relative to that of activated silica gel at 3439  $\text{cm}^{-1}$  (Fig. 1a), representing the obvious interactions between hydroxyl with strong polarity and benzene rings with weak polarity. The results of FT-IR confirmed that the non-covalent imprinted film was successfully introduced onto the surface of silica gel based on sol-gel process.

Fig. 2 shows the SEM images of activated silica gel (a), non-imprinted silica gel (b) and imprinted silica gel (c). As displayed, the MIPs contained pores embedded in the network while NIPs had a relatively smooth surface. Moreover, by BET analysis, the specific surface area of MIPs was attained of 289.1  $\text{m}^2 \text{g}^{-1}$ , higher than that of NIPs (270.2  $\text{m}^2 \text{g}^{-1}$ ) and activated silica gel (265.8  $\text{m}^2 \text{g}^{-1}$ ). So, the coating of imprinted film on the activated silica gel increased the specific surface area by using PAHs to create the polymeric microstructure, and thereby could accelerate mass transfer and improve adsorption capacity.

### 3.2. Evaluation of adsorption properties

Adsorption properties of the MIPs were evaluated by carrying out equilibrium binding experiments in artificial seawater samples. The binding kinetics of the imprinted silica gel sorbents for PAHs was examined. It is observed from Fig. 3, that the amounts of PAHs adsorbed onto MIPs increased with time and nearly reached saturation state within 10 h; adsorption rate rapidly increased within 7.5 h and then slowly increased approximating level off. The high adsorption rate can be ascribed to the preferential and rapid adsorption of PAHs onto the recognition sites in the MIPs. When these imprinted sites were occupied, it became difficult for PAHs to implant into the MIPs. This would cause the adsorption rate to slow down. Although NIPs displayed similar trend to MIPs on the PAHs adsorption, as seen in Fig. 3, their adsorption capacity was much lower. The equilibrium adsorption capacity for PAHs onto MIPs within 10 h was 2.7  $\text{mg g}^{-1}$ , while only 1.2  $\text{mg g}^{-1}$  onto the corresponding NIPs. This might be likely because of the non-specific adsorption of NIPs, due to the absence of imprinting procedure and thereafter lacking suitable recognition sites and imprinting cavities in the NIPs. In contrast, interestingly, there were a number of precise imprinting sites in the MIPs, resulting in specific adsorption, and thus they produced higher adsorption capacity.

The isotherm of Langmuir–Freundlich (LF) equation was considered for evaluating binding characteristics of the synthetic MIPs [37]. Experimental data were fitted in LF, and the relationship between concentrations of bound ( $B$ ) and free guests ( $F$ ) was established as.

$$B = \frac{N_t \alpha F^m}{1 + \alpha F^m}$$

where,  $N_t$  is the total number of binding sites,  $\alpha$  is related to the median binding affinity constant ( $K_0$ ) via  $K_0 = \alpha^{1/m}$ , and  $m$  is the heterogeneity index which will be equal to 1 for a homogeneous material, or will take values within 0 and 1 if the material is heterogeneous. In order to estimate the  $N_t$ ,  $K_0$  and  $m$  values, the isotherm data ( $F$  and  $B$ ) were successfully fitted

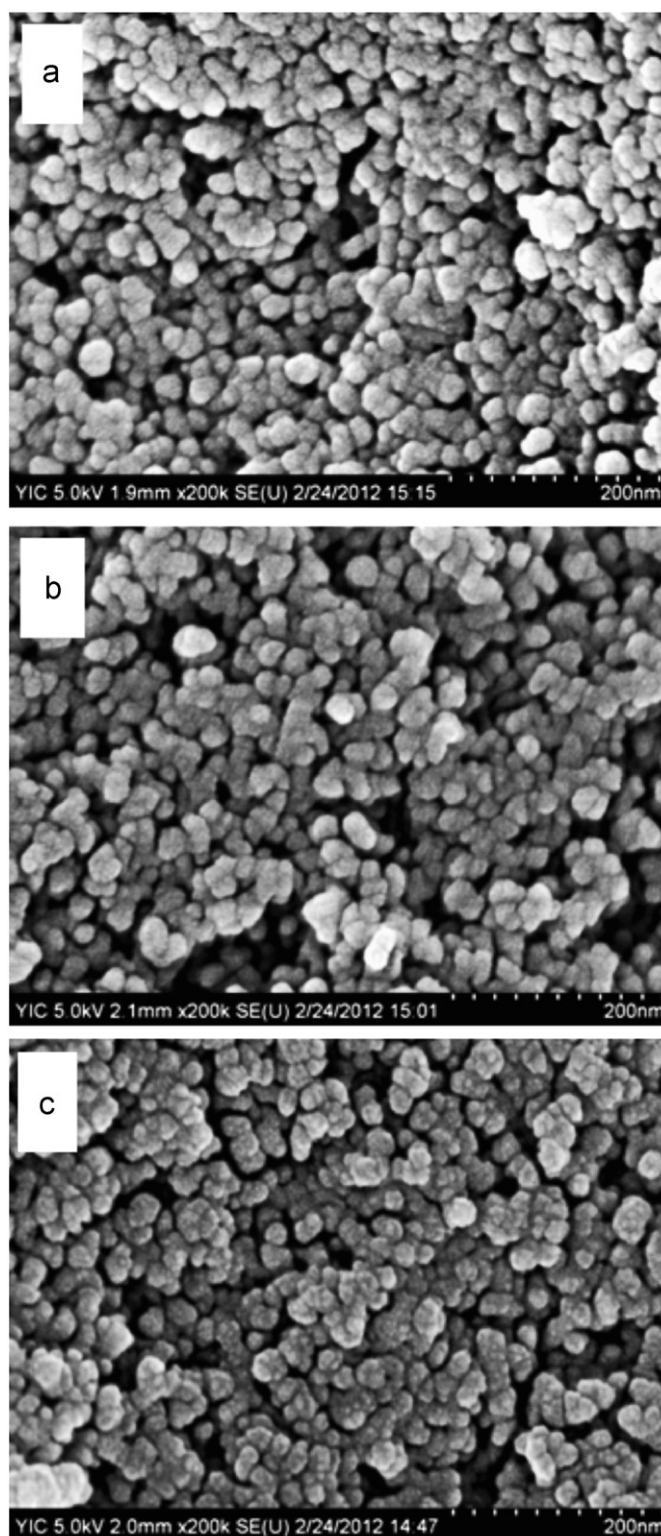


Fig. 2. FT-IR spectra of (a) activated silica gel, (b) non-imprinted silica gel and (c) imprinted silica gel.

according to the LF model (Fig. 4), and the resultant fitting coefficients are listed in Table 1. As shown in Table 1, the value of  $m$  demonstrated the higher degree of binding site heterogeneity of MIPs with the index ( $m=0.64$ ) than that of NIPs ( $m=0.80$ ). However, the MIPs had the higher concentration of binding sites per gram of polymers ( $N_t=3031.3 \mu\text{g g}^{-1}$ ) and median binding affinity ( $K_0=40.64 \mu\text{g g}^{-1}$ ). The results indicated that the binding

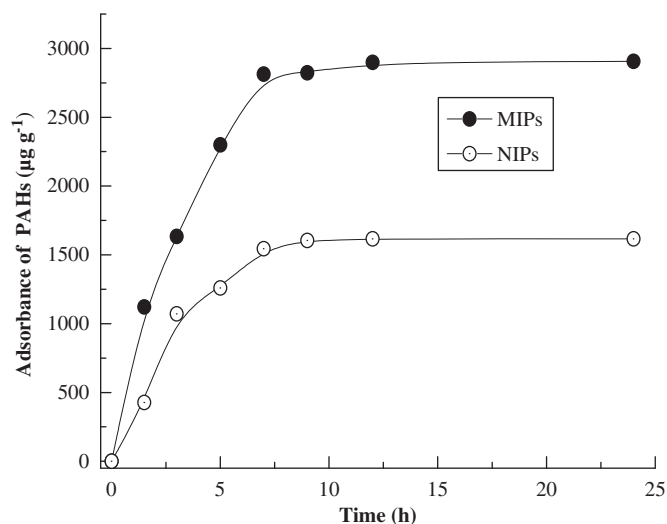


Fig. 3. Kinetic adsorption of PAHs onto MIPs and NIPs. Experimental conditions:  $V=10.0$  mL;  $C_0=1$   $\mu\text{g L}^{-1}$ ; mass of polymer, 50 mg.

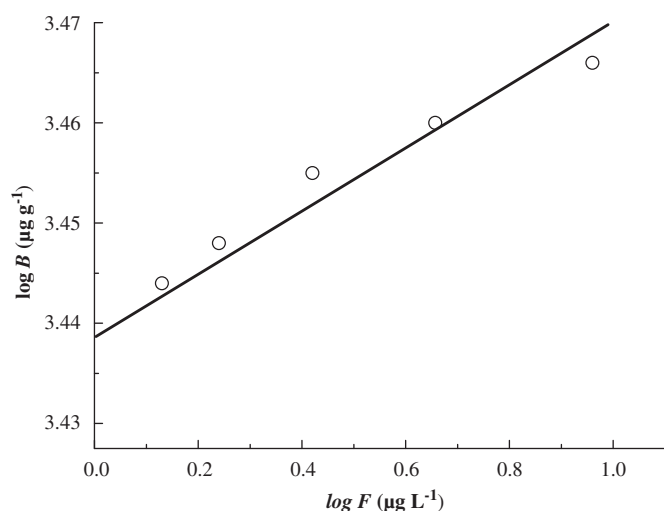


Fig. 4. Binding isotherm and Langmuir–Freundlich model fitting for MIPs. Experimental conditions:  $V=10.0$  mL; mass of polymer, 50 mg; adsorption time, 24 h.

Table 1

LF isotherm model fitting coefficients for MIPs and NIPs.

Polymers	Isotherm parameters				$R^2$
	$N_t/\mu\text{gg}^{-1}$	$a/\text{g}\mu\text{g}^{-1}$	$m$	$K_0^a/\text{g}\mu\text{g}^{-1}$	
MIPs	3031.3	10.75	0.64	40.64	0.9968
NIPs	1667.9	3.78	0.80	5.27	0.9967

<sup>a</sup> The median binding affinity constant was calculated as  $K_0=\alpha^{1/m}$ .

capacity of the MIPs was much higher than that of the NIPs. Additionally, the plot exhibited saturation at higher concentrations, demonstrating the excellent imprinting effect due to a number of specific binding sites on MIPs.

### 3.3. Binding selectivity of the MIPs for PAHs

Generally, the cavities of imprinted sorbent created by the imprinted molecules can lead to much greater affinity for the template molecule, in comparison with non-imprinted sorbent. In several batch experiments, the distribution ratio ( $K_d$ ) was

calculated using the following equation.

$$K_d = \frac{(F_0 - F_t)V}{F_t m}$$

where,  $V$ ,  $F_0$ ,  $F_t$  and  $m$  represent the volume of the solution (mL), solution concentrations before and after adsorption ( $\mu\text{g L}^{-1}$ ) and mass of the polymer ( $\mu\text{g}$ ), respectively.

The imprinting factor (IF) is defined as.

$$IF = \frac{K_{d,MIP}}{K_{d,NIP}}$$

To evaluate the selectivity of the synthesized MIPs, the uptake capacities of the sorbent for 16 PAHs were tested, rebinding experiments were performed using a 16 PAHs mixture with the initial concentration of  $1$   $\mu\text{g L}^{-1}$ , and the distribution ratios ( $K_d$ ), equilibrium adsorption ( $B$ ) and IF were calculated. As seen from Table 2, the  $K_d$  for the 16 PAHs on the MIPs were from 0.78 to  $1.77$   $\text{L g}^{-1}$ ; in contrast, the  $K_d$  on the NIPs were from 0.37 to  $0.99$   $\text{L g}^{-1}$ . When compared to NIPs for PAHs, the MIPs have 1.5–3.1 fold IF in seawater medium. The MIPs showed high selectivity due to the tailor-made cavity selective for PAHs. The adsorbance of individual PAH to MIPs was found in the range of  $111.0$  to  $195.0$   $\mu\text{g g}^{-1}$  after adsorption equilibrium.

Interestingly, the higher IF was exhibited for line type structural PAHs including Nap, Acy, Ace, Flu, Ant, Py, BaA, Ipy, BbF, DahA and BghiP, in contrast with angle type ones including Fl, Phe, Chr, BaP and BkF. Additionally, the results also showed that the binding capacity of BbF to MIPs was the highest ( $195.0$   $\mu\text{g g}^{-1}$ ), whereas the least one was that of Fl ( $111.0$   $\mu\text{g L}^{-1}$ ). Considering the properties of lower/higher hydrophobia ( $K_{ow}$  value was 4.18 for Fl, and 6.323 for BbF), the molecular steric type of angle (Fl) and line (BbF) might explain their lower and higher binding capacity of specific interactions in MIPs for Fl and BbF, respectively. Although there are no pronounced functional groups in PAHs, the imprinting process can be performed via special non-covalent interactions between functional monomers and PAHs, i.e. the hydrophobic interaction and  $\pi$ - $\pi$  interaction resulted from the aromatic ring structure of PAHs. Furthermore, it is obvious that the aromatic ring seems to be important for molecular recognition, and the imprinting effect decreased with the angle increase of the angle type PAHs (such as Fl, Phe, Flu, Chr, and BaP). The configurations of the angle type (Fl and Phe) and line type (Ant) were optimized, resulting in the

Table 2

Distribution ratio ( $K_d$ ), adsorption capacity ( $B$ ), imprinting factor (IF) of MIPs and NIPs, and octanol/water partition coefficient ( $\log K_{ow}$ ) for PAHs.

PAHs	MIPs			NIPs		$\log K_{ow}^a$
	$K_d/\text{Lg}^{-1}$	$B/\mu\text{gg}^{-1}$	IF	$K_d/\text{Lg}^{-1}$	$B/\mu\text{gg}^{-1}$	
Nap	1.31	184.2	3.12	0.42	59.2	3.3
Acy	1.77	194.7	2.19	0.81	89.8	4.0
Ace	0.86	125.8	2.32	0.37	53.7	3.92
Fl	0.78	111.0	1.90	0.41	57.8	4.18
Phe	1.64	176.3	1.91	0.86	92.5	4.45
Ant	1.64	185.1	2.10	0.78	87.4	4.46
Flu	1.37	170.0	2.21	0.62	76.3	5.16
Py	1.51	185.6	2.40	0.63	77.5	5.18
BaA	1.66	187.1	2.13	0.78	87.4	5.91
Chr	1.62	172.2	1.84	0.88	93.5	5.86
BbF	1.76	195.0	2.17	0.81	89.3	6.32
BkF	0.99	119.3	1.50	0.66	79.8	6.45
BaP	1.76	177.2	1.78	0.99	99.5	6.04
Ipy	1.64	182.9	2.08	0.79	88.3	6.58
DahA	1.48	181.4	2.35	0.63	77.7	6.86
BghiP	1.35	167.7	2.21	0.61	75.9	6.58
$\Sigma$ PAHs	1.31	2716	3.12	0.42	1285	/

<sup>a</sup>  $\log K_{ow}$  octanol/water partition coefficient.

lowest energy, by using Hartree–Fock (HF) method with 6–31G basis set [38]. As shown in Fig. 5, the results demonstrated that the angle type structured molecules such as Fl and Phe in cyclobenzene had lower electron densities than that of line type ones such as Ant, theoretically. So, the concept of “multiple molecule imprinting” proposed by Krupadam et al [28] was also successfully demonstrated by using the 16 PAHs mix as a template. The formed binding cavities have different binding pocket energies and even smaller molecule may loosely trap in the MIPs but energetically favorable molecule fit properly.

### 3.4. Matrix effects

Because of the possible strong interference in the trace level PAHs detection caused by presence of other high dissolved matters, it is necessary to study the effect of organic matter and inorganic common ions on the MIPs adsorption for PAHs in

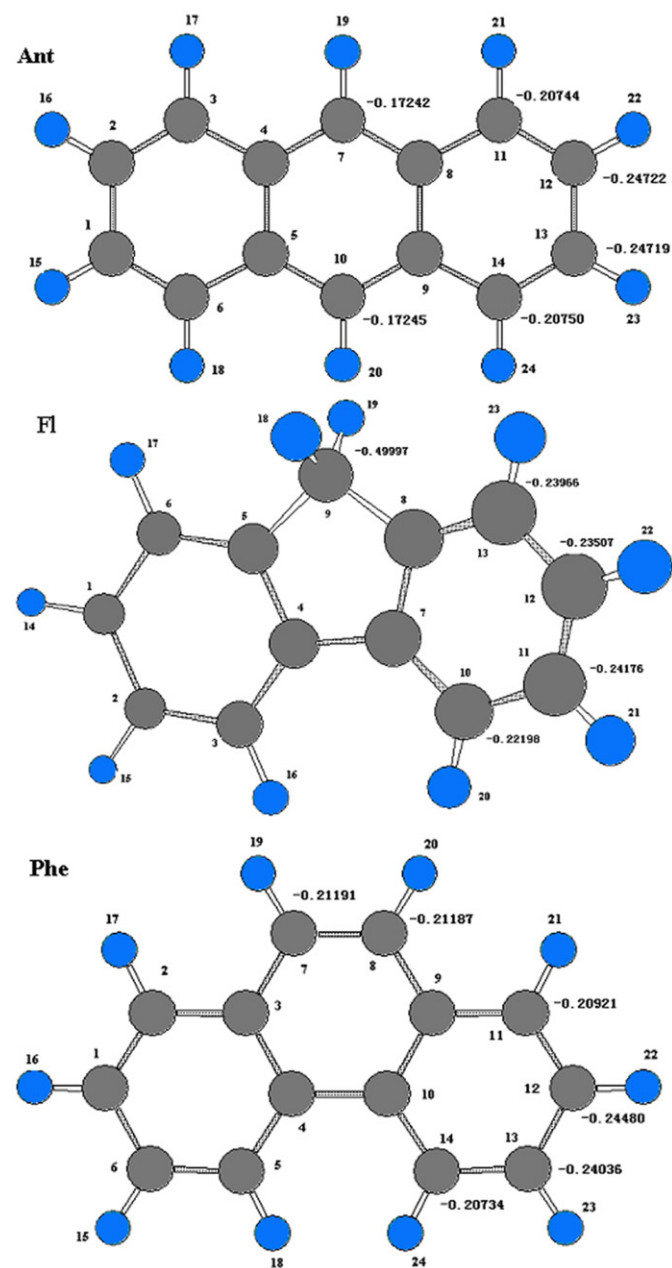


Fig. 5. Optimized configurations and natural charge analysis of Fl, Ant and Phe derived by Hartree–Fock method with 6–31G basis set.

seawater samples, and thereby to evaluate the adsorption capacity of MIPs for PAHs. The observations of matrix effects were shown in Table 3. By using artificial seawater spiked with individual PAH at  $1 \mu\text{g L}^{-1}$  and humic acid (HA) at  $12 \text{ mg L}^{-1}$  for testing the influence of dissolved organic matter (DOM), the results revealed that higher level DOM caused a strong interference in trace level detection of specific environmental pollutants [39]. Effects of inorganic common ions such as  $\text{Ca}^{2+}$ ,  $\text{Mg}^{2+}$  and  $\text{Fe}^{3+}$  on the adsorption capacity of MIPs were also studied because of their universal existence in environmental samples. In artificial seawater, the MIPs binding affinity for PAHs quickly declined at higher concentrations of  $\text{Mg}^{2+}$  and  $\text{Fe}^{3+}$  compared to that of  $\text{Ca}^{2+}$ . The results showed that the inorganic cations at higher valence (such as  $\text{Fe}^{3+}$ ) or with smaller ionic radius at same valency (such as  $\text{Mg}^{2+}$ ) might have the higher polarizability. For ions with the same charges, such as  $\text{Mg}^{2+}$  (ionic radius as  $0.065 \text{ nm}$ ) and  $\text{Ca}^{2+}$  (ionic radius as  $0.099 \text{ nm}$ ), smaller ion has larger charge density and larger coulombic force; for ions with different charges, such as  $\text{Ca}^{2+}$  and  $\text{Fe}^{3+}$  (ionic radius as  $0.064 \text{ nm}$ ), higher charge ion has higher charge density. As a result, the MIPs showed diminished adsorption of PAHs when increasing total dissolved ions in environmental samples. Therefore, it is significant and imperative to eliminate the matrix effects for sensitive and accurate determination of PAHs. Excitedly, the binding characteristics of the presented MIPs were still far superior to other MIPs for PAHs reported [23,28,40], and should be sufficient for extracting/removing PAHs present at trace level from natural seawater, as shown 93.2% in Table 3.

On the other hand, as shown in Table 3, the presence of NaCl at a high concentration even 3% had no obvious effect on adsorption, giving 98.1% efficiency. Salting can enhance extraction of some compounds from water [41]. As is well known that, natural seawater usually contains 2.7% NaCl. So it is reasonable to use the 3% NaCl solution to investigate the matrix effects.

### 3.5. MISPE applications to seawater sample for PAHs analysis

The applicability of the developed MIPs as SPE sorbent was tested by GC–MS for analysis of PAHs in environmental water samples. To demonstrate the applicability and reliability of MIPs, the spiked standard PAHs seawater samples were cleaned up with MIPs. Natural seawater collected from Zhanshan Beach (Qingdao, China) and artificial seawater were spiked with  $1 \mu\text{g L}^{-1}$  PAHs mixture. A pre-weighed amount of 50 mg of MIPs or NIPs were added into the empty SPE columns, respectively, and then a 10 mL of seawater sample was filtered, and the SPE column was washed with 10 mL of methanol/acetic (1:1, v/v). As seen from Table 4, the recoveries of all the 16 PAHs were higher than 82%; the matrix had no significant influence. For the natural seawater samples, the recoveries were in the range of 83–113% with the

Table 3

Interference study of environmental parameters- $\text{Ca}^{2+}$ ,  $\text{Mg}^{2+}$ ,  $\text{Fe}^{3+}$  and HA for PAHs adsorption onto MIPs.

Solvent spiked with $1 \mu\text{g L}^{-1}$ PAHs	Environmental parameters				$\Sigma$ PAHs adsorbed on MIPs/%
	$\text{Ca}^{2+}/\text{mol L}^{-1}$	$\text{Mg}^{2+}/\text{mol L}^{-1}$	$\text{Fe}^{3+}/\text{mol L}^{-1}$	HA/ $\text{mg L}^{-1}$	
3%NaCl(aq)	–	–	–	–	98.1
3%NaCl(aq)	0.065	0.053	–	–	86.5
3%NaCl(aq)	0.51	–	–	–	85.8
3%NaCl(aq)	–	–	0.51	–	53.7
3%NaCl(aq)	–	0.51	–	–	56.1
3%NaCl(aq)	–	–	–	12.00	47.4
Natural seawater	0.05	0.05	$9.82 \times 10^{-8}$	3.7	93.2



**Table 4**  
Method recoveries, precision, and LOD for PAHs in seawater ( $n=3$ )<sup>a</sup>.

PAHs	Artificial seawater <sup>b</sup>			Natural seawater <sup>c</sup>		
	Recoveries /%	RSD/%	LOD/ng L <sup>-1</sup>	Recoveries /%	RSD/%	LOD /ng L <sup>-1</sup>
Nap	94	5.8	6.9	95	3.2	6.1
Acy	98	4.5	4.3	89	3.5	6.5
Ace	90	6.4	9.5	85	3.8	6.8
Fl	91	4.2	5.9	90	4.2	5.2
Phe	90	4.5	5.0	83	4.5	5.4
Ant	92	2.3	2.1	95	3.2	6.3
Flu	100	3.9	6.1	113	3.9	7.9
Py	96	4.6	6.3	95	4.8	7.6
BaA	95	5.1	4.3	98	5.1	7.1
Chr	92	4.9	9.5	89	4.9	10.5
BbF	98	5.7	9.9	101	3.7	8.9
BkF	90	5.7	9.2	85	6.3	11.2
BaP	97	5.1	8.2	95	7.1	10.2
IPy	91	6.1	8.8	96	7.5	9.6
DahA	90	5.7	5.9	99	6.9	6.8
BghiP	96	6.1	7.2	91	7.2	12.6
∑PAHs	98	5.9	7.2	92	6.9	8.9

<sup>a</sup> Extraction conditions: sample volume, 10 mL; extraction solvent: 10 mL acetone: DCM (2:1, v/v); extraction time, 5 min; centrifugation time: 8 min; extraction temperature 20 °C.

<sup>b</sup> Artificial seawater (Subow) constituents: NaCl, 26.518 g L<sup>-1</sup>; CaCl<sub>2</sub>, 0.725 g L<sup>-1</sup>; MgCl<sub>2</sub>, 2.447 g L<sup>-1</sup>; NaHCO<sub>3</sub>, 0.202 g L<sup>-1</sup>; MgSO<sub>4</sub>, 3.305 g L<sup>-1</sup>; NaBr, 0.083 g L<sup>-1</sup>; spiked with 1 μg L<sup>-1</sup> PAHs.

<sup>c</sup> Obtained from Zhanshan beach of Qingdao of China.

relative standard deviation (RSD) of 3.2–7.5% (Table 4), which indicated the MISPE was applicable for selective extraction of PAHs from real water samples. The limit of detection ( $S/N=3$ ) for natural seawater was calculated of 5.2–12.6 ng L<sup>-1</sup>. The detection limit value is much lower than the maximum contaminant level for all PAHs in drinking water, namely 0.2 μg L<sup>-1</sup> stipulated standard value by the United States EPA. It should be noted that general validation with certified reference materials of seawater is most significant and obligatory as has been done in case of marine sediments [42]. Merely, now for us, it is impossible to obtain the required certified reference materials of seawater. Still, the developed MISPE–GC–MS was validated practically applicable in seawater analysis for PAHs.

#### 4. Conclusions

A novel material of MIPs was prepared via sol–gel process and used as SPE adsorbent to successfully extract 16 PAHs from seawater samples, presenting robust binding capacity, favorable detection sensitivity and satisfactory recovery and precision. The present imprinting mode opens attractive perspectives for the development of MIPs-based systems for emerging environmental pollutants like endocrine disrupting chemicals especially POPs. Such systems could be invaluable for the rapid analytical control of such compounds in environmental pollution monitoring and remediation.

#### Acknowledgments

This work was supported by The National Natural Science Foundation of China (21105117, 20975089, 21107057), The Natural Science Foundation of Shandong Province of China (Y2007B38, ZR2010BQ027), The Department of Science and Technology of Shandong Province of China (2010GSF10222), The Innovation Projects of the Chinese Academy of Sciences (KZCX2-EW-206, KZCX2-YW-223, KZCX2-YW-Q07-04), The Yantai Research and Development Program (2010158, 2007323), the CAS/SAFEA International Partnership Program for Creative

Research Teams, and the 100 Talents Program of the Chinese Academy of Sciences.

#### References

- [1] International Program on Chemical Safety (IPCS), World Health Organization, Geneva, 1998.
- [2] K. Prevedouros, E. Brorstrom-Lunden, J.C. Halsall, K.C. Jones, R.G.M. Lee, A.J. Sweetman, *Environ. Pollut.* 128 (2004) 17.
- [3] R.G. Harvey, *Polycyclic Aromatic Hydrocarbons*, John Wiley & Sons, New York, 2010.
- [4] P. Plaza-Bolanos, A.G. Frenich, J.L.M. Vidal, *J. Chromatogr. A* 1217 (2010) 6303.
- [5] M. Hyder, L.L. Aguilar, J. Genberg, M. Sandahl, C. Wesen, J.A. Jonsson, *Talanta* 85 (2011) 919.
- [6] M.R. Ras, F. Borrull, R.M. Marce, *Trend. Anal. Chem.* 28 (2009) 347.
- [7] M. Farre, S. Perez, C. Goncalves, M.F. Alpendurada, D. Barcelo, *Trend. Anal. Chem.* 29 (2010) 1347.
- [8] A. Beltran, F. Borrull, P.A.G. Cormack, R.M. Marce, *Trend. Anal. Chem.* 29 (2010) 1363.
- [9] X.L. Song, J.H. Li, C.Y. Liao, L.X. Chen, *Chromatographia* 74 (2011) 89.
- [10] J.P. Ma, R.H. Xiao, J.H. Li, J.B. Yu, Y.Q. Zhang, L.X. Chen, *J. Chromatogr. A* 1217 (2010) 5462.
- [11] J.P. Ma, M. Li, J.H. Li, C.J. Rui, Y.P. Xin, L.X. Chen, *J. Chromatogr. Sci.* 49 (2011) 683.
- [12] O. Kruger, G. Christoph, U. Kalbe, W. Berger, *Talanta* 85 (2011) 1428.
- [13] A.J. King, J.W. Readman, J.L. Zhou, *Anal. Chim. Acta* 523 (2004) 259.
- [14] J.H. Li, Z.W. Cai, S.F. Xu, C.Y. Liao, X.L. Song, L.X. Chen, *J. Liq. Chromatogr. Related Technol.* 34 (2011) 1578.
- [15] F. Gosetti, U. Chiominatto, E. Mazzucco, E. Robotti, G. Calabrese, M.C. Gennaro, E. Marengo, *J. Chromatogr. A* 1218 (2011) 6308.
- [16] F. Galan-Cano, V. Bernabe-Zafon, R. Lucena, S. Cardenas, J.M. Herrero-Martinez, G. Ramis-Ramos, M. Valcarcel, *J. Chromatogr. A* 1218 (2011) 1802.
- [17] X.L. Song, J.H. Li, J.T. Wang, L.X. Chen, *Talanta* 80 (2009) 694.
- [18] L.X. Chen, S.F. Xu, J.H. Li, *Chem. Soc. Rev.* 40 (2011) 2922.
- [19] M.B. Gholivand, M. Khodadadian, *Talanta* 85 (2011) 1680.
- [20] S.F. Xu, J.H. Li, L.X. Chen, *Talanta* 85 (2011) 282.
- [21] S.F. Xu, L.X. Chen, J.H. Li, W. Qin, J.P. Ma, *J. Mater. Chem.* 21 (2011) 12047.
- [22] S. Marx, A. Zaltsman, *Int. J. Environ. Anal. Chem.* 83 (2003) 671.
- [23] J.P. Lai, R. Niessner, D. Knopp, *Anal. Chim. Acta* 522 (2004) 137.
- [24] C. Baggiani, L. Anfossi, P. Baravalle, C. Giovannoli, G. Giraudi, *Anal. Bioanal. Chem.* 389 (2007) 413.
- [25] F.L. Dickert, P. Achatz, K. Halikus, *Fresen. J. Anal. Chem.* 371 (2001) 11.
- [26] X.L. Song, Z.R. Lian, J.T. Wang, *Sinic-Environ. Chem.* 31 (2012) 9.
- [27] R.J. Krupadam, B. Bhagat, S.R. Wate, G.L. Bodhe, B. Sellergren, Y. Anjaneyulu, *Environ. Sci. Technol.* 43 (2009) 2871.
- [28] R.J. Krupadam, M.S. Khan, S.R. Wate, *Water Res.* 44 (2010) 681.
- [29] R.J. Krupadam, B. Bhagat, M.S. Khan, *Anal. Bioanal. Chem.* 397 (2010) 3097.
- [30] S.F. Xu, J.H. Li, L.X. Chen, *J. Mater. Chem.* 21 (2011) 4346.
- [31] Y. Li, W.H. Zhou, H.H. Yang, X.R. Wang, *Talanta* 79 (2009) 141.

- [32] G.Z. Fang, J. Tan, X.P. Yan, *Anal. Chem.* 77 (2005) 1734.
- [33] Y.Y. Wen, J.H. Li, W.W. Zhang, L.X. Chen, *Electrophoresis* 32 (2011) 2131.
- [34] J.H. Li, W.H. Lu, J.P. Ma, L.X. Chen, *Microchim. Acta* 175 (2011) 301.
- [35] R. Zhu, W.H. Zhao, M.J. Zhai, F.D. Wei, Z. Cai, N. Sheng, Q. Hu, *Anal. Chim. Acta* 658 (2010) 209.
- [36] A.L.P. Silva, K.S. Sousa, A.F.S. Germano, V.V. Oliveira, J.G.P. Espínola, M.G. Fonseca, C. Airoidi, T. Arakaki, L.N.H. Arakaki, *Colloids Surf. A* 332 (2009) 144.
- [37] R.J. Umpleby, S.C. Baxter, Y. Chen, R.N. Shah, K.D. Shimizu, *Anal. Chem.* 73 (2001) 4584.
- [38] M.B. Gholivand, M. Khodadadian, F. Ahmadi, *Anal. Chim. Acta* 658 (2010) 225.
- [39] X.L. Song, J.H. Li, L.X. Chen, Z.W. Cai, C.Y. Liao, H.L. Peng, H. Xiong, *J. Braz. Chem. Soc.* 23 (1) (2012) 132.
- [40] R.J. Krupadam, R. Ahuja, S.R. Wate, *Sens Actuators B* 124 (2007) 444.
- [41] K. Jinno, T. Muramatsu, Y. Saito, Y. Kiso, S. Magdic, J. Pawliszyn, *J. Chromatogr. A* 754 (1996) 137.
- [42] V. Fernandez-Gonzalez, E. Concha-Grana, S. Muniategui-Lorenzo, P. Lopez-Mahia, D. Prada-Rodriguez, *J. Chromatogr. A* 1196–1197 (2008) 65.